# Steering the outcome of a photochemical reaction – an *in-silico* experiment on the $H_2CSO$ sulfine using few-femtosecond dump pulses

Benoit Mignolet[1,*] and Basile F. E. Curchod[2]
[1] *Theoretical Physical Chemistry, Research Unit Molecular Systems, B6c, University of Liège, B4000, Liège, Belgium*
[2] *Department of Chemistry, Durham University, South Road, Durham DH1 3LE, United Kingdom.*
[*] *Email: bmignolet@uliege.be*

We propose a pump-dump control scheme using sub-10fs pulses to enhance the photochemical formation of the three-membered C-S-O ring oxathiirane from the parent $H_2CSO$ sulfine molecule. The ultrashort nature of the pulses is essential to promptly alter the photoinduced dynamics, *e.g.* while a bond is elongating, which is key to selectively form the oxathiirane by radiative dumping. We carried out an *in-silico* pump-dump experiment with excited-state dynamics simulations that include the interaction with electric field of the pump and dump pulses. By applying the dump pulse when the CS bond is elongating, the population transferred to the ground state will form the oxathiirane with a branching ratio of 4, much higher than the one solely due to nonradiative relaxation (0.66). The overall oxathiirane yield can be increased by up to 17% when the 6fs IR dump pulse is applied at a delay time of 47fs.

In photochemistry, the nonradiative relaxation of photoexcited molecules mostly occurs through the succession of one or several conical intersections[1-4] (CIs). They correspond to regions of the potential energy surface (PES) where two electronic states intersect, *i.e.*, become degenerate, and provide highly-efficient nonradiative decay pathways. Following photoexcitation, a nuclear wavepacket evolving on the PES of an excited electronic state may reach regions of the nuclear configuration space that would be inaccessible on the ground state due to high-energy barriers. If there is a conical intersection in these regions connecting the excited and the ground state, the nuclear wavepacket can relax nonradiatively and form photoproducts that, in some cases, differ from the ones produced by thermal processes. Hence, the number of photoproducts formed, and their respective yield, is governed by the CIs of the molecule accessed during the excited-state dynamics. Pump-dump schemes[5, 6] bypass the need of CIs to induce relaxation to the ground state by using stimulated emission. As the coupling with an external electric field relies on the electronic transition dipole moment, pump-dump strategies offer the possibility to transfer the nuclear wavepacket back to the ground-state at any time during the excited-state dynamics – and not just around a CI. In this Communication, we propose a light-induced dumping mechanism to enhance the formation of a targeted photoproduct using a few-femtosecond pulse that is short enough to interact with the molecule during half a vibrational period. Using the $H_2CSO$ sulfine molecule as an example, we show with excited-state dynamics simulations, including explicitly the interaction with the laser pulses, that a dumping induced when the CS bond is elongating leads to the selective formation of one of the photoproducts on the ground state.

Pump-dump experiments have traditionally been carried out on molecules with femtosecond pulses having a duration longer than 50fs.[7-11] With the recent development of attosecond science,[12-14] sub-10fs have been used to monitor ultrafast nuclear rearrangements,[15-17] sometimes using a delayed pulse that dumps the wavepacket to another electronic state where dissociation can occur – a strategy employed to probe the excited-state dynamics. The ultrashort nature of these pulses is highly desirable for the pump-dump experiments proposed here for two reasons. First, the enhancement of a targeted photoproduct yield relies on the fact that the nuclear wavepacket is highly localized in space. This requires to (*i*) photoexcite the molecule with a short fs pulse so that the wavepacket launched on the excited state is narrow, (*ii*) dump the population with a short fs pulse that addresses the wavepacket when it is localized in a specific region of the PES, and while the wavepacket is not too spread out on the PES. Second, the short pulse duration implies that the stringent resonance condition between the energy gap and the pulse carrier frequency is somehow relaxed, as short pulses typically have bandwidths of several tenths of eV (see Fig. 1f).

We investigated the effect of the pump-dump control scheme on the photochemistry of the $H_2CSO$ sulfine molecule[18] (Fig. 1a), as it has been recently reported that its photoproducts, formed on the ground state, depend on how the nuclear wavepacket approaches the first CI region and when the nonradiative decay takes place.[19] Upon photoexcitation to the $S_1$ state, the nuclear wavepacket relaxes and reaches a strong nonadiabatic region after 50fs, where it can relax either towards the sulfine ground state minimum or the oxathiirane one (Fig. 1a). The fate of the wavepacket on the ground state $S_0$ strongly depends on how it has approached the nonadiabatic region. If the CS bond is elongating and CSO angle decreasing when the wavepacket is transferred to $S_0$, the oxathiirane molecule will be formed on $S_0$. On the other hand, the nonradiative decay will lead to the reformation of the original sulfine molecule if the wavepacket approaches the CI with a simultaneous contraction of the CS bond and increase of the CSO angle[19] (Fig. 1c and 1d). This observation indicates that there is a strong correlation between the dynamics of the nuclear wavepacket when it enters the region of strong nonadiabatic coupling (NAC) and the products formed on the ground state. More importantly, the nonradiative transitions responsible for the formation of oxathiirane happens sooner (between 45 and 60fs) than the ones leading to the regeneration of sulfine (60 to 75fs). Such a temporal difference between the two processes constitutes an ideal case to apply the pump-dump control scheme mentioned above. As it takes 40fs for the photoexcited molecule to perform a full oscillation of the CS bond, it is crucial to apply short few-fs pulses to selectively interact with nuclear wavepacket. By utilizing the dump pulse after around 45fs following photoexcitation – when the CS bond is elongating and CSO angle decreasing – the oxathiirane molecule should be formed on the ground electronic state (see schematic representations in Fig. 1b).

**Theory:** A vast majority of previous pump-dump simulations carried out on polyatomic molecules did not include explicitly all the nuclear degrees of freedom during the excited-state dynamics, including the effect of the pulse.[20, 21] In this work, we modeled a whole pump-dump experiment, from the photoexcitation by the pump pulse to the nonradiative relaxation to $S_0$, including the dumping induced by the delayed pulse. For this purpose, we used the eXternal Field *Ab Initio* Multiple Spawning method[22, 23] (XFAIMS) that is based on the trajectory-guided method AIMS.[24-26] Since the pump and dump pulses contain only a few cycles, it is important to include their effect in the simulations because (*i*) the amplitude transferred from one electronic state to another strongly depends on the pulse waveform and the form of the initial nuclear wavepacket and (*ii*) slightly off-resonant transitions can occur.[27] In XFAIMS, the nuclear wavepackets on each electronic state are represented by a set of coupled trajectory basis functions (TBFs) that are propagated classically using electronic-structure information computed on-the-fly, here using

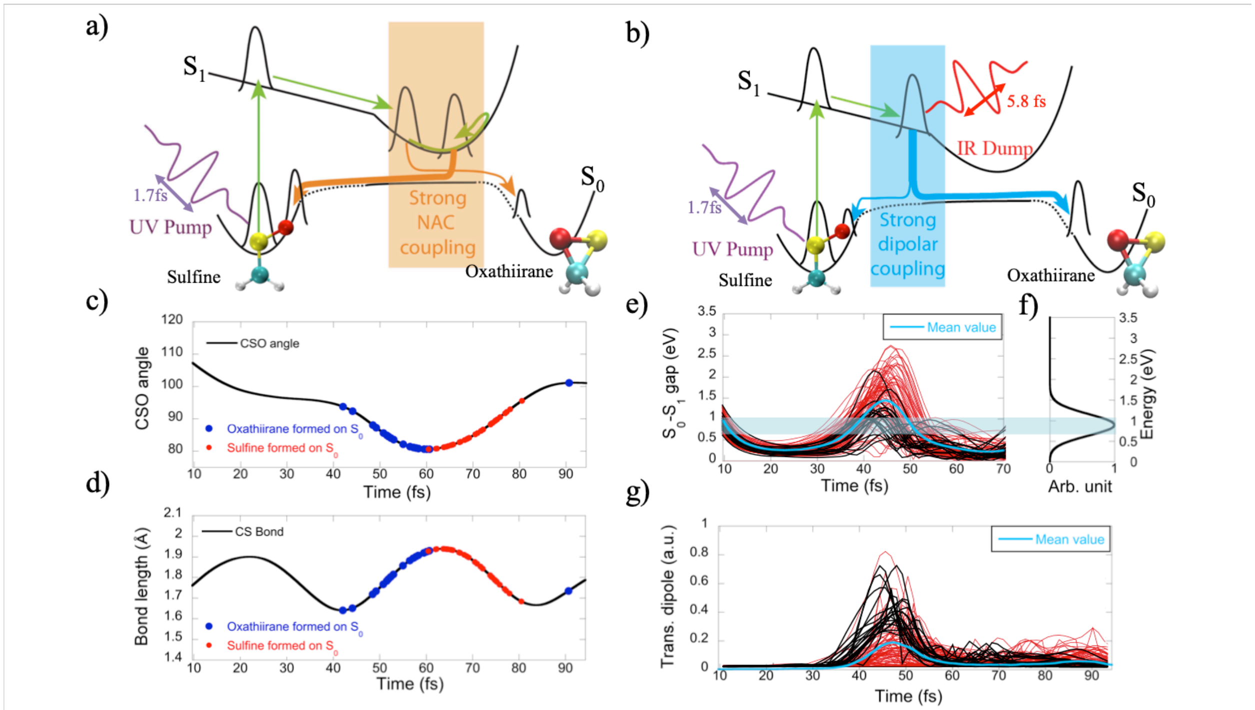

Fig. 1. a) Schematic representation of the sulfine photochemistry following photoexcitation to the $S_1$ state by a 1.7fs resonant UV pump pulse (z polarization $\vec{\varepsilon}_1 = (0,0,1)$ , $f_{0,1} = 0.03\text{a.u.}$ , $\omega_1 = 0.12\text{a.u.}$ , $\sigma_1 = 30\text{a.u.}$ (FWHM=1.7fs ), and $CEP_1 = 0$ ). The molecule is planar in the x-y plane while the z axis is pointing out of the page. Once relaxed to $S_0$, 39% of the photoexcited population forms the oxathiirane product (thin orange arrow) while 61% comes back to the sulfine ground state (tick orange arrow). b) Schematic representation of the pump-dump experiment. The pump pulse is the same as in panel (a) while the dump pulse parameters are as follows: x polarization $\vec{\varepsilon}_2 = (1,0,0)$ , $f_{0,2} = 0.03\text{a.u.}$ , $\omega_2 = 0.03\text{a.u.}$ , $\sigma_2 = 100\text{a.u.}$ (FWHM=5.8fs) and $CEP_2 = \pi / 2$ . Depending on when the dump pulse is applied, more oxathiirane or sulfine can be selectively formed on $S_0$ (represented by the thickness of the arrows). c) Mean CSO angle during the excited-state dynamics. The blue and red dots represent the nonadiabatic transfer of population from $S_1$ to $S_0$ leading to the formation on $S_0$ of the oxathiirane or the sulfine molecule, respectively. As long as the CSO angle decreases, a transfer of population to $S_0$ leads to the formation of oxathiirane. As soon as the CSO angle starts to increase, a transfer of population to $S_0$ will regenerate the sulfine. d) Same as panel (c), but for the CS bond stretching. e) The mean $S_0$-$S_1$ energy gap is shown (blue line) during the excited-state dynamics triggered by the pump pulse of panel (a), along with the energy gap of the 90 simulations carried out. Black lines correspond to initial conditions for which the dump pulse with a delay time of 47fs induces a dumping of at least 10% of the photoexcited population. For red lines, the $S_1 \rightarrow S_0$ dumping is lower than 10%. f) Fourier transform of the dump pulse. The blue area indicates the energy region that is within the bandwidth of the dump pulse. g) Same as panel (e), but for the *x* component of the $S_1$-$S_0$ transition dipole moment. The *y* and *z* components of the $S_1$-$S_0$ transition dipole moment are at least twice smaller than the *x* component.

MOLPRO.[28, 29] The number of TBFs is changing in time, as new TBFs can be spawned whenever strong nonadiabatic (CI) or dipolar (pulse) couplings are encountered. The dynamics of the amplitude carried by each TBF is obtained by integrating the time-dependent Schrödinger equation, in which the molecular Hamiltonian contains the NACs as well as the dipolar couplings with the electric field of the pulses. In the simulations, we used a combination of two Gaussian-shaped pulses leading to the pump and the dump pulses. The pulses are defined from the time-derivative of the vector potential and the sine term at the end of Eq. (1) ensures that the integral of $\mathbf{E}(t)$ is 0 at the end of the pulse, as required by Maxwell's equations.[30]

$$\mathbf{E}(t)=\sum_{i=1}^{2}\varepsilon_i f_{0,i}\exp\left[\frac{-\left(t-t_{0,i}\right)^2}{2\sigma_i^2}\right]\left(\cos\left(\omega_i\left(t-t_{0,i}\right)+CEP_i\right)-\frac{\sin\left(\omega_i\left(t-t_{0,i}\right)+CEP_i\right)\left(t-t_{0,i}\right)}{\omega_i\sigma_i^2}\right) \quad (1)$$

where the index *i* runs over the sequence of pulses, $\boldsymbol{\varepsilon}_i$ is the polarization vector, $f_{0,i}$ the field strength, $\omega_i$ is the carrier frequency, $\sigma_i$ the pulse duration (FWHM=2.3 $\sigma_i$ ) and $CEP_i$ is the carrier envelope phase (see Fig. 1 for details). The waveform of few-cycle pulses, which depends on the CEP, strongly affects the photoexcitation/dumping efficiency.[27] Therefore the waveform of the pump and dump pulses is the same for all the pump-dump delays in Eq. 1.

**Computational details:** The dynamical simulations are carried out from the ground electronic state for a set of 90 initial conditions sampled from a classical Boltzmann distribution. The reactant ($H_2CSO$ sulfine) is a planar molecule oriented according to its moment of inertia, *i.e.* with the *x* and *y* axes in the molecular plane and the *z* axis perpendicular to it. The dynamical simulations are carried out for oriented molecules and the electronic structure is computed at each time step at the SA2-CASSCF(4/3)/6-31G(d) level. The spawning procedure for field-induced coupling in XFAIMS induces the spawn of one child TBFs per parent TBFs already present in the simulation when the pulse is applied.[22] Since the pulses are short, a good overlap between the parent and the child TBFs is achieved during the pulses duration. Once the pulse is over, the TBFs evolving on $S_0$ without being coupled to other TBFs are removed from the simulations after 5fs. This limits the number of TBFs in the simulations, but it also implies that once the pump pulse is over the TBFs on $S_0$ will be discarded from the simulations before the dump pulse is applied, which is an approximation. However, 4 IR photons from the dump pulse would be required to photoexcite the molecule from $S_0$ to $S_1$ in the Franck-Condon region, which is unlikely to occur in comparison to the dumping process that is a one-photon process. The dump pulse could also potentially photoexcite the $S_1$ wavepacket to a higher excited state ($S_2$), but the average $S_1$-$S_2$ energy gap is at least twice as large as the $S_1$-$S_0$ energy gap when the dump pulse is applied, meaning that the dumping process should largely dominate.

The dump pulses are applied for time delays where the system will also suffer strong NACs. However, the spawning mechanism differs for the two different processes. For nonradiative relaxation, the kinetic energy of the newly-spawned child TBFs is rescaled to ensure total energy conservation.[25] Since nonadiabatic transitions usually occur over a range of energy gaps between the two coupled states,[4] the momenta of the parent and child TBFs differ and their overlap at the spawning point may not be exactly equal to 1.0. For field-induced spawning, the momentum of the child and parent TBFs are not modified and kept the same,[22] and their the overlap is therefore equal to 1.0 at the spawning point. Therefore, we differentiate the child TBFs spawned due to the NAC and due to the electric field. The child TBFs spawned due to the nonadiabatic coupling are coupled to the parent TBFs solely by the NAC and the child TBFs spawned due to the electric field are coupled to the parent TBFs solely by the dipolar coupling. These child TBFs can, however, in turn spawn new TBFs due to NAC or dipolar coupling.

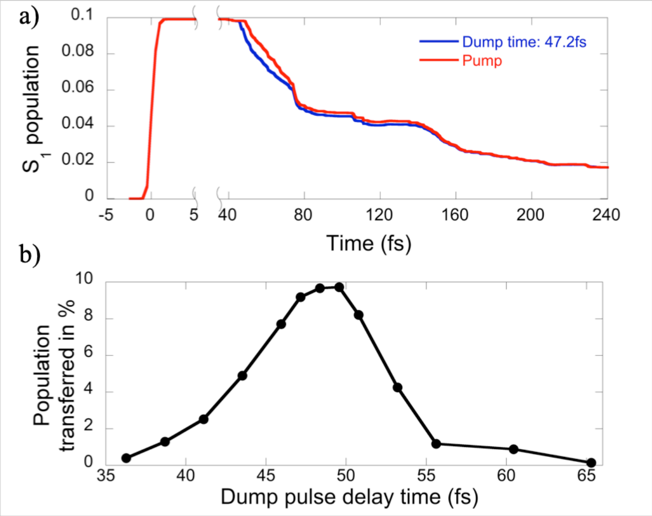

Fig. 2: a) $S_1$ population for excited-state dynamics simulations including the pump pulse solely (red curve), or including a combination of pump and dump pulses with a delay of 47fs (blue curve). b) Population transferred from $S_1$ to $S_0$ by the dump pulse as a function of the pump-dump delay. The population transferred is evaluated 5fs after the dump pulse is applied: $\left[S_{1pop}^{\text{Pump only}}(\tau+5)-S_{1pop}^{\text{Pump dump }\tau}(\tau+5)\right]/S_{1pop}^{\text{Pump only}}(\tau+5)$ , where τ is the delay time.

**Results and discussion:** The first stage of the *in silico* pump-dump experiment is the photoexcitation of the sulfine molecule from its ground electronic state by a short and resonant UV pump pulse (see Fig. 1a) that promptly promotes about 10% of population to the $S_1$ state (Fig. 2a). Then, the nuclear wavepacket formed on $S_1$ starts evolving on the excited PES and, if there is no dump pulse, will relax nonradiatively to the ground state at later times. The excited-state dynamics simulations indicate that the wavepacket first reaches a region of strong nonadiabatic coupling after around 60fs of dynamics, where a large transfer of population to $S_0$ occurs, and then suffers a slower population decay (Fig. 2a). Following the nonradiative relaxation, most of the wavepacket goes back to the sulfine ground state (61%) while the other part (39%) forms the oxathiirane photoproduct. The current simulations carried out at the CASSCF level agree with earlier MS-CASPT2 simulations.[19] It should be pointed out that the nonradiative relaxation leads to rich ground state chemistry, not described here, in which other products are formed such as dissociated molecules. As the yield of these dissociated molecules is directly proportional to yield of oxathiirane formed,[19] measuring the amount of dissociated molecules as a function of the pump-dump delay could be used experimentally to test the efficiency of this control scheme.

We aim at enhancing the oxathiirane yield by applying a delayed pulse that would transferred back population from $S_1$ to $S_0$ around 47fs, when the CS bond is stretching and CSO angle is decreasing, that is, when a transfer of population to the ground state should lead to the formation of oxathiirane (Fig. 1c and d). The efficiency of the dumping relies on the matching condition between the $S_0$-$S_1$ energy gap with the pulse carrier frequency (1500nm, see Fig. 1f), and on the magnitude of the transition dipole moment, whose $x$-component reaches a maximum 47fs after the photoexcitation process (Fig. 1g). For a pump-dump delay of 47fs, the dump pulse induces a significant $S_1 \rightarrow S_0$ transfer of amplitude for 24% of the initial conditions, leading to a total transfer of 9.2% of the photoexcited $S_1$ population to $S_0$ (see Fig. 2a). The TBFs that are significantly affected by the dump pulses are those with the largest transition dipole moments (Fig. 1g) and an energy gap matching the laser bandwidth (Fig. 1f). The overall population transferred to $S_0$ by the dump pulse varies with the pump-dump delay: it peaks for delay times around 47fs and is close to zero for delay times shorter than 40fs or longer than 55fs (Fig. 2b). The latter observation is due to the fact that, for these delay times, the transition dipole moments are close to zero and the energy gaps are off-resonant with the laser carrier frequency (Fig. 1e and 1f). The $S_1$ population trace 100fs after the dump pulse is the same with or without the dump pulse (Fig. 2a), indicating that the dump pulse induced a transfer of population that should have anyway relaxed to $S_0$, but nonradiatively without the second pulse. Since the products formed by the dumping mechanism differ from the ones induced by the nonradiative relaxation, the asymptotic yield should differ with the dump pulse.

Once the wavepacket has relaxed to the $S_0$, the oxathiirane molecule is formed with a yield depending on the pump-dump delay. For a delay time of 47fs, the oxathiirane population is increased by 36% once the wavepacket has gone through the conical intersection for the first time, 120fs after the photoexcitation by the pump (Fig. 3a). This demonstrates the efficiency of the dump pulse to significantly enhance the oxathiirane yield. At later times, once the $S_1$ nuclear wavepacket has almost completely relaxed to $S_0$ (after 240fs), the increase of oxathiirane population stabilizes at around 17% (Fig. 3a). The increase of oxathiirane with the pump-dump delay (Fig. 3b) follows overall the $S_1 \rightarrow S_0$ population transfer (Fig. 2b). However it should be pointed out that the conversion efficiency, *i.e.*, the dumped population that leads to the oxathiirane formation, depends on the momentum of the wavepacket when reaching the ground state. If the radiative relaxation occurs when the CSO angle decreases and the CS bond elongates (Fig. 1c-d), the oxathiirane will be formed on $S_0$. Furthermore the dumping must occur when the CSO angle is lower than 90°, otherwise the wavepacket is too close to the Franck-Condon region and the sulfine is formed back on $S_0$. For delays around 47fs, the conversion efficiency to form the oxathiirane is about 80%, twice larger than when the molecule relaxes nonradiatively. Combined to the fact that the population dumped by the delayed pulse does not relax nonradiatively, it leads to a significant increase in the oxathiirane population, achieving the goal of the pump-dump protocol proposed here.

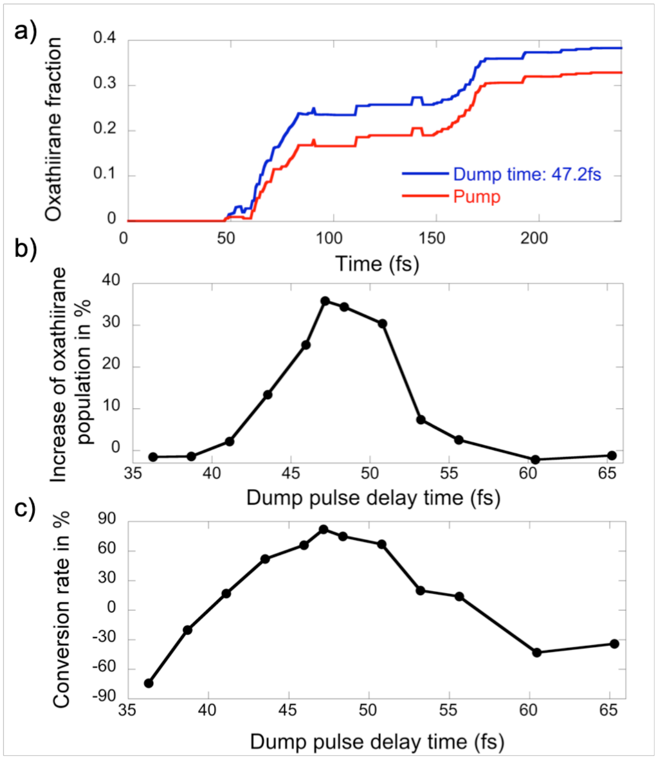

Fig. 3: a) Fraction of the $S_1$ population converted in oxathiirane on $S_0$ for dynamical simulations including the pump pulse solely (red curve) and including a combination of pump and dump pulses with a delay time of 47fs (blue curve). b) Increase of the oxathiirane population 120fs after the photoexcitation ($\left(Y_{Oxa}^{\text{Pump dump }\tau}(120) - Y_{Oxa}^{\text{Pump}}(120)\right) / Y_{Oxa}^{\text{Pump}}(120)$ ) as a function of the pump-dump delay. c) Conversion efficiency computed as $\dfrac{Y_{Oxa}^{\text{Pump dump }\tau}(120) - Y_{Oxa}^{\text{Pump}}(120)}{S_{1pop}^{\text{Pump only}}(\tau+5) - S_{1pop}^{\text{Pump dump }\tau}(\tau+5)}$ , where τ is the pump-dump delay. Positive values correspond to an increase of oxathiirane population, while negative values correspond to an increase of sulfine population (and therefore decrease of oxathiirane population).

In the simulations above, we consider an oriented molecule and used an ultrashort few-cycle pump pulse and dump pulse that is tailored to induce a large dumping effect. Producing few-cycle IR[31-33] and UV[34] pulses is now experimentally possible, but we note that longer pulses could also be used for the present application as long as they can address the wavepacket evolving on $S_1$ when the CS bond is elongating, *i.e.*, within a time-window of 15fs. Molecular orientation[35-37] can be achieved for instance by combining one and two-color non-resonant femtosecond laser pulses[37] but it still remains challenging. The control scheme proposed here does not rely on a prior molecular orientation. For the sulfine, the $y$ and $z$ components of the $S_0$-$S_1$ transition dipole moment are at least twice lower than the $x$ component when the dump pulse is applied. Hence, if the molecules are not oriented there will be a decrease of the dumping efficiency of about 2/3 and so a lower increase of the oxathiirane population, but the overall effect of the pump-dump process will still be significant.

**Conclusions:** In this Communication, we demonstrated the possibility to enhance the yield of a given photoproduct using a delayed few fs pulse. This pulse dumps the excited-state nuclear wavepacket towards the ground state when it approaches specifically the region of intersection, leading to the formation of the targeted product. Even if only a small fraction of the $S_1$ wavepacket is transferred back to $S_0$ by the dump pulse (10% here), it is sufficient to generate a significant increase of the targeted product population for this example employing a sulfine molecule. The dumping scheme proposed here, therefore, offers an efficient way of enhancing the yield of a minor photoproduct.

**Acknowledgments:** B.M. acknowledges support from the Fonds National de la Recherche Scientifique, Belgium (F.R.S.-FNRS) and the University of Liège. Computational resources have been provided by the Consortium des Equipements de Calcul Intensif (CECI), funded by the F.R.S.-FNRS under Grant No. 2.5020.11. This work also made use of the facilities of the Hamilton HPC Service of Durham University.

**References**

1. W. Domcke and D. R. Yarkony, Annual Review of Physical Chemistry **63** (1), 325-352 (2012).
2. W. Domcke, D. R. Yarkony and K. Horst, *Conical intersections: electronic structure, dynamics and spectroscopy*. (World Scientific, 2004).
3. G. A. Worth and L. S. Cederbaum, Annual Review of Physical Chemistry **55** (1), 127-158 (2004).
4. B. G. Levine and T. J. Martínez, Annu. Rev. Phys. Chem. **58**, 613-634 (2007).
5. R. Kosloff, S. A. Rice, P. Gaspard, S. Tersigni and D. J. Tannor, Chemical Physics **139** (1), 201-220 (1989).
6. D. J. Tannor, R. Kosloff and S. A. Rice, The Journal of chemical physics **85** (10), 5805-5820 (1986).
7. D. Polli, P. Altoè, O. Weingart, K. M. Spillane, C. Manzoni, D. Brida, G. Tomasello, G. Orlandi, P. Kukura, R. A. Mathies, M. Garavelli and G. Cerullo, Nature **467**, 440 (2010).
8. Z. Kuang, Q. Guo, X. Wang, H. Song, M. Maroncelli and A. Xia, The journal of physical chemistry letters **9** (15), 4174-4181 (2018).
9. E. Papagiannakis, M. Vengris, D. S. Larsen, I. H. M. Van Stokkum, R. G. Hiller and R. Van Grondelle, The Journal of Physical Chemistry B **110** (1), 512-521 (2006).
10. D. S. Larsen, I. H. M. van Stokkum, M. Vengris, M. A. van der Horst, F. L. de Weerd, K. J. Hellingwerf and R. van Grondelle, Biophysical journal **87** (3), 1858-1872 (2004).
11. G. Vogt, P. Nuernberger, T. Brixner and G. Gerber, Chemical physics letters **433** (1-3), 211-215 (2006).
12. M. Nisoli, P. Decleva, F. Calegari, A. Palacios and F. Martín, Chemical Reviews **117** (16), 10760-10825 (2017).
13. C. Francesca, S. Giuseppe, S. Salvatore, V. Caterina and N. Mauro, Journal of Physics B: Atomic, Molecular and Optical Physics **49** (6), 062001 (2016).
14. F. Krausz and M. Ivanov, Rev. Mod. Phys. **81** (1), 163-234 (2009).
15. W. K. Peters, D. E. Couch, B. Mignolet, X. Shi, Q. L. Nguyen, R. C. Fortenberry, H. B. Schlegel, F. Remacle, H. C. Kapteyn, M. M. Murnane and W. Li, Proceedings of the National Academy of Sciences **114** (52), E11072-E11081 (2017).
16. A. Ludwig, E. Liberatore, J. Herrmann, L. Kasmi, P. López-Tarifa, L. Gallmann, U. Rothlisberger, U. Keller and M. Lucchini, The Journal of Physical Chemistry Letters **7** (10), 1901-1906 (2016).
17. G. Sansone, F. Kelkensberg, J. F. Perez-Torres, F. Morales, M. F. Kling, W. Siu, O. Ghafur, P. Johnsson, M. Swoboda, E. Benedetti, F. Ferrari, F. Lepine, J. L. Sanz-Vicario, S. Zherebtsov, I. Znakovskaya, A. L/'Huillier, M. Y. Ivanov, M. Nisoli, F. Martin and M. J. J. Vrakking, Nature **465** (7299), 763-766 (2010).
18. P. R. Schreiner, H. P. Reisenauer, J. Romanski and G. Mloston, Journal of the American Chemical Society **132** (21), 7240-7241 (2010).
19. B. Mignolet, B. F. E. Curchod and T. J. Martínez, Angewandte Chemie International Edition **55** (48), 14993-14996 (2016).
20. R. Mitrić, M. Hartmann, J. Pittner and V. Bonačić-Koutecký, The Journal of Physical Chemistry A **106** (44), 10477-10481 (2002).
21. K. Hoki, L. González and Y. Fujimura, The Journal of chemical physics **116** (6), 2433-2438 (2002).
22. B. Mignolet, B. F. E. Curchod and T. J. Martínez, *The Journal of Chemical Physics* **145** (9), 191104 (2016).
23. B. Mignolet and B. F. E. Curchod, The Journal of Chemical Physics **148** (13), 134110 (2018).
24. M. Ben-Nun and T. J. Martınez, The Journal of chemical physics **108** (17), 7244-7257 (1998).

25. M. Ben-Nun and T. J. Martínez, Adv. Chem. Phys. **121**, 439-512 (2002).
26. B. F. E. Curchod and T. J. Martínez, Chemical Reviews **118** (7), 3305-3336 (2018).
27. B. Mignolet, B. F. E. Curchod, F. Remacle and T. J. Martínez, The Journal of Physical Chemistry Letters **10** (0), 742-747 (2019).
28. B. G. Levine, J. D. Coe, A. M. Virshup and T. J. Martínez, Chemical Physics **347** (1–3), 3-16 (2008).
29. H.-J. Werner, P. J. Knowles, F. R. Manby, M. Schuetz, P. Celani, G. Knizia, T. Korona, R. Lindh, A. Mitrushenkov, G. Rauhut, T. B. Adler, R. D. Amos, A. Bernhardsson, A. Berning, D. L. Cooper, M. J. O. Deegan, A. J. Dobbyn, F. Eckert, E. Goll, C. Hampel, A. Hesselmann, G. Hetzer, T. Hrenar, G. Jansen, C. Koeppl, Y. Liu, A. W. Lloyd, R. A. Mata, A. J. May, S. J. McNicholas, W. Meyer, M. E. Mura, A. Nicklass, P. Palmieri, K. Pflueger, R. Pitzer, M. Reiher, T. Shiozaki, H. Stoll, A. J. Stone, R. Tarroni, T. Thorsteinsson, M. Wang and A. Wolf, *MOLPRO a package of ab initio programs*. (Cardiff, UK, 2009).
30. L. B. Madsen, Physical Review A **65** (5), 053417 (2002).
31. F. Süßmann, S. Zherebtsov, J. Plenge, N. G. Johnson, M. Kübel, A. M. Sayler, V. Mondes, C. Graf, E. Rühl and G. G. Paulus, Review of Scientific Instruments **82** (9), 093109 (2011).
32. N. G. Johnson, O. Herrwerth, A. Wirth, S. De, I. Ben-Itzhak, M. Lezius, B. Bergues, M. F. Kling, A. Senftleben and C. D. Schröter, Physical Review A **83** (1), 013412 (2011).
33. H. Timmers, Y. Kobayashi, K. F. Chang, M. Reduzzi, D. M. Neumark and S. R. Leone, Optics Letters **42** (4), 811-814 (2017).
34. M. Y. Shverdin, D. R. Walker, D. D. Yavuz, G. Y. Yin and S. E. Harris, Physical review letters **94** (3), 033904 (2005).
35. H. Stapelfeldt and T. Seideman, Reviews of Modern Physics **75** (2), 543 (2003).
36. M. Spanner, S. Patchkovskii, E. Frumker and P. Corkum, Physical Review Letters **109** (11), 113001 (2012).
37. P. M. Kraus, D. Baykusheva and H. J. Wörner, Physical review letters **113** (2), 023001 (2014).